ELECTROMAGNETIC EMISSIONS TO 60 GHZ FROM A BPT-4000 EDM HALL THRUSTER

Edward J. Beiting and James E. Pollard
The Aerospace Corporation
Los Angeles, California

Vadim Khayms and Lance Werthman
Lockheed Martin Space Systems Company
Sunnyvale, California

ABSTRACT

Radiated electric and magnetic fields, static magnetic fields, discharge oscillations, and conducted emissions were measured from a BPT-4000 Engineering Development Model (EDM) Hall thruster operating with a flight-like power processing unit (PPU) and xenon flow controller. Measurements were made at four operating conditions: a power of 3.0 kW with 300 V discharge voltage, 3.0 kW at 400 V, 4.5 kW at 300 V, and 4.5 kW at 400 V. Only 4.5 kW data are reported here. Radiated electric fields were measured from 10 kHz to 18 GHz following MIL-STD 461E RE102 specifications and from 18 to 60 GHz with a 1 MHz (3 dB) bandwidth. Radiated ac magnetic fields were measured from 30 Hz to 300 kHz using MIL-STD 461D RE101 specifications at three orthogonal field directions to the side and back of the thruster. Three-axis static magnetic fields were measured at 12 positions around the thruster with only the magnets energized and under normal thruster operating conditions. Conducted emissions were measured between the PPU and the bus simulator from 30 Hz to 50 MHz following 461C CE01 and CE03 specifications. Anode current oscillation was measured between 1 kHz and 100 MHz through the anode cable operating with the PPU, through the anode cable operating with a laboratory power supply, and through the power cable bundle operating with the PPU.

INTRODUCTION

In an effort to increase payload capability of the future commercial and military spacecraft, a program was initiated at Lockheed Martin several years ago to investigate Hall Current Thruster (HCT) technology. Over the last three years Lockheed Martin and Aerojet have collaborated on the development of the flight versions of the BPT-4000 Hall thruster, a power processing unit (PPU), and a Xenon flow controller (XFC). In parallel with the development of flight hardware, Lockheed Martin has pursued a number of integration studies. The main emphasis of this comprehensive Hall Thruster Propulsion System (HTPS) development and integration program has been to gain quantitative information on the effects of the ionized thruster plume on various spacecraft subsystems and to help mitigate risk associated with the introduction of this new propulsion technology on future spacecraft.

Hall Current Thrusters are electromagnetic devices that accelerate ionized particles and produce thrust by reaction. In the process of their operation, due to the intrinsic plasma oscillations and instabilities, Hall thrusters generate electromagnetic emissions, which can interfere with the operation of on-board equipment. Electromagnetic Compatibility (EMC) studies are performed to evaluate the interaction of radiated emissions with critical spacecraft components and to assess acceptability of a Hall Current Thruster propulsion system for commercial and military applications. The major concern appears to be verification that the radiated electric field emissions from the HCT will not desensitize spacecraft receivers. Aside from the receivers, other spacecraft hardware undergoes radiated susceptibility testing to ensure compatible operation. Therefore, a direct measurement of radiated emissions is needed to evaluate the impact of the HCT operation on the noise levels in spacecraft communication links.

A comprehensive set of tests was performed on an engineering development model of the BPT-4000 at the Aerospace Corporation EMC facility a) to characterize and measure radiated electric field, magnetic field, and conducted emissions over the frequency range of interest, b) to obtain the spectrum of thruster current oscillations and c) to measure static magnetic field profile in the vicinity of the thruster. The data were taken

with the thruster operating with a flight-like power processing unit (PPU) and xenon flow controller (XFC) over a range of operating conditions, varying both power levels and discharge voltages to cover the entire flight envelope. This paper describes the details of the test setup, discusses representative data, and presents some conclusions drawn from the results of the test.

FACILITY AND CONFIGURATION

The Aerospace Corporation EMC facility comprises three components. The first is a small, all-dielectric vacuum tank that houses the thruster. This fiberglass tank is largely transparent to electromagnetic radiation and mates to a stainless steel vacuum chamber that has a nominal pumping speed of 220,000 liter/sec. The second component, a semi-anechoic room, surrounds the dielectric tank to shield the thruster from the ambient electromagnetic environment. This metallic room is lined with 0.6 m high pyramids that absorb radiation from the thruster at frequencies higher than 80 MHz to mitigate reflections from the walls of the room. The final component is a set of calibrated receivers that records the radiation emanating from the thruster. Below 18 GHz, the receiver connects sequentially to a series of antennas through a panel in the semi-anechoic room using a two-section semi-rigid cable with known attenuation. The arrangement of these components is shown in Figure 1. Above 18 GHz, a smaller receiver situated in the anechoic room connects sequentially through one of two short cables to a series of octave horns.

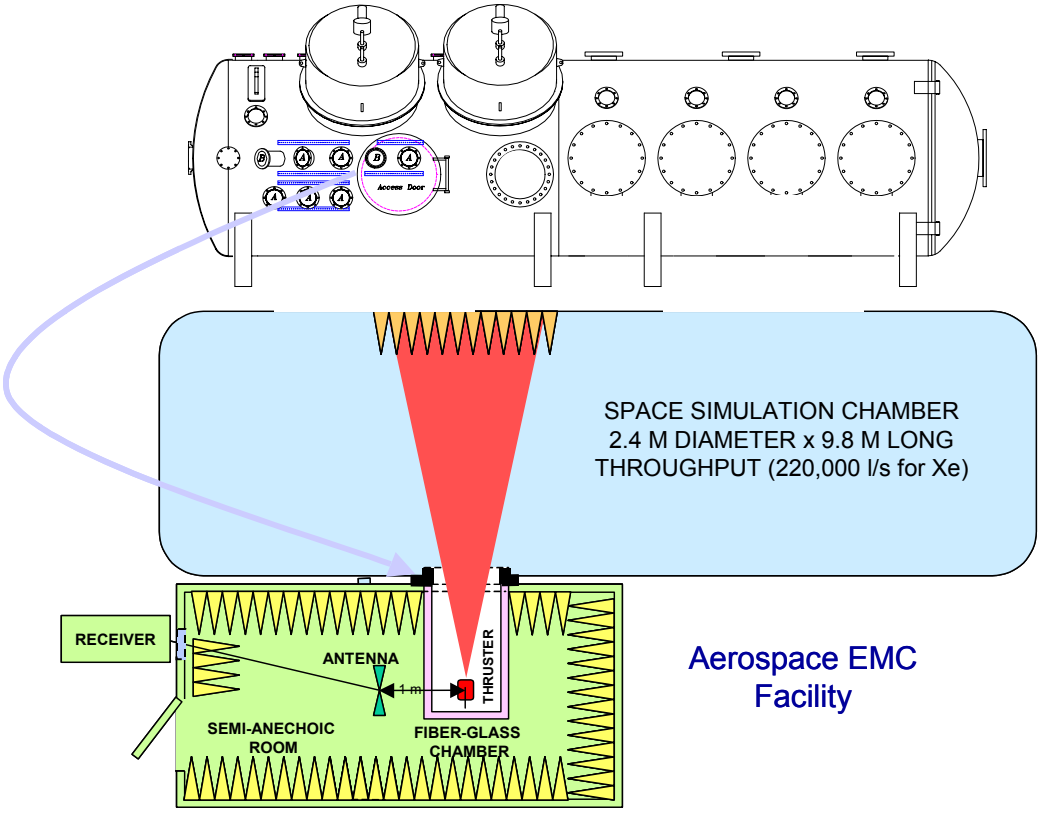

Figure 1. Layout of the facility used to measure electromagnetic emissions from the BPT-4000 thruster.

Ambient radiation leaks into the main vacuum tank through openings and cables attached to equipment in the tank. Subsequently, this radiation leaks in the anechoic room through the fiberglass tank orifice and is especially apparent in the 20 –200 MHz frequency band where there is room resonance. This radiation was reduced about 10 dB by covering the opening of the fiberglass tank with a carbon fiber mesh with 5 cm x 5 cm openings. The plume of the thruster exhausts through this mesh into the main vacuum tank and terminates on a beam dump comprising an array of 0.6 m high aluminum pyramids that are covered with flexible graphite to reduce sputtering by high energy ions. The pyramidal design of this conducting beam dump serves to reduce scattering of electromagnetic radiation from the thruster by the main tank at frequencies greater than 80 MHz.

The small anechoic room and the fiberglass vacuum chamber distort the electromagnetic spectrum emitted from a thruster. This is true for all semi-anechoic rooms for frequencies were the pyramids do not absorb the radiation reflected from the wall. A metallic room with cross sectional dimensions of 3 x 3 m is expected to have resonant frequencies near 50 MHz. Filling the enclosure with absorbing pyramids lowers the Q of the room which increases the bandwidth and lowers the resonant frequencies. The 0.6 m anechoic pyramids have a quarter wavelength that corresponds to a frequency of 125 MHz and most effectively absorb radiation above this frequency. Measured correct terms vary between –30 and +30 dB and are stronger for vertically polarized receiving antennas than horizontally polarized antennas but are significant for both polarizations.

At frequencies above 200 MHz, the pyramids effectively absorb the reflections from the walls and the anechoic room perturbations become negligible. However, at frequencies above 1 GHz, interference effects and absorption from the wall of the fiberglass become non-negligible. The transmission coefficient of an S2 fiberglass wall of 1 cm thickness undergoes sinusoidal oscillations with a period of 7.5 GHz. This indicates that periodically the radiation measured outside the chamber is too low by 2.3 – 3.0 dB. The room correction terms and the calculated transmission through the fiberglass wall are shown in Figure 2. Additional information on the EMC facility has been published [1].

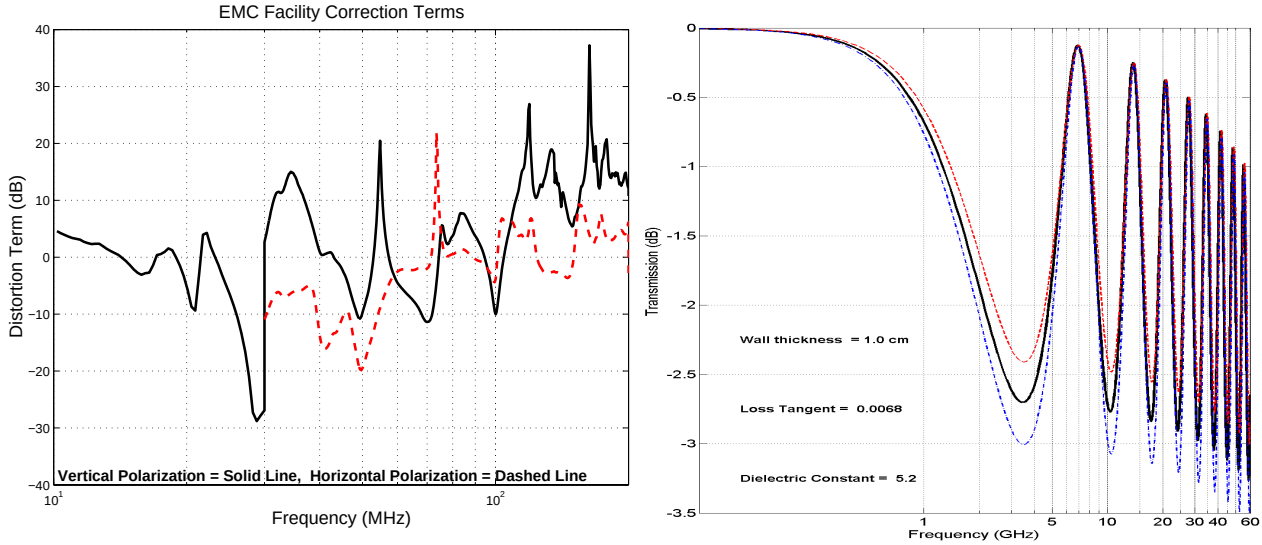

Figure 2. EMC anechoic room correction terms for vertical and horizontally polarized receiving antennas (left) and calculated transmission of fiberglass chamber (right).

TABLE 1

Background Pressure for BPT-4000 Operating at 4.5 kW

Thruster Voltage (V)	Thruster Current (A)	Propellant Flow (mg/s)	Ion Gauge (Torr)	Corrected Pressure (Torr)
300	15.0	15.41	4.41×10^{-5}	1.53×10^{-5}
400	11.3	12.62	3.78×10^{-5}	1.31×10^{-5}

The thruster was attached to a 12.7 mm (0.5") thick aluminum "L" bracket. This bracket was mounted with good thermal contact on a 203 x 203 mm (8" x 8") water-cooled aluminum shelf positioned so the centerline of the thruster coincided with the centerline of the fiberglass tank. This shelf remained below 25°C for all operating conditions. Propellant lines were routed along the bottom of the dielectric chamber underneath a fiberglass plate to a vacuum feed-through in the main chamber. The distance from the fiberglass back flange to the back of the vertical mounting plate was 47 mm and to the front of the horizontal mounting plate 230 mm. Pressures measured in the main chamber for the operating conditions reported here are given in Table 1. The corrected pressure is 0.348 times the indicated pressure. The pressures behind the thruster in the fiberglass tank are typically a factor of 2.4 – 2.7 times those measured in the main chamber.

EMISSION

Instrument Configuration

The bands, resolution bandwidths (RBW), low noise (pre)amplifiers (LNAs), and antennas used for the radiated emission measurements are listed in Table 2. The wavelengths and maximum dimensions of the antennas are used to calculate the far field distance given the last column in this table. All antennas were placed 1 meter to the side of the thruster as shown in Figure 1. Essentially, below 1 GHz, the antennas are in the near field and above this frequency they are in far field. Both vertically and horizontally polarized emission data were acquired for all antennas with the exception of the active rod that is used only in the vertical orientation.

TABLE 2
Electromagnetic Band Parameters

Bands	Wavelength Ranges	RBW (kHz)*	LNA	Antenna	L (m)	Far Field Distance**
10 - 150 kHz	30 - 2 km	1	None	Active Rod	1	90 - 6 km
0.15 - 30 MHz	2000 – 10 m	10	None	Active Rod	1	6000 – 30 m
30 - 200 MHz	10 - 1.5 m	100	HP4740	Biconical	1.5	30 - 4.5 m
0.2 - 1 GHz	1.5m – 30 cm	100	HP4740	Log Periodic	0.85	4.5 – 4.8m
1 - 2 GHz	30 – 15 cm	1000	HP4740	DR Horn	0.2	90 – 54 cm
2 - 18 GHz	15 - 1.67 cm	1000	Miteq 1	DR Horn	0.2	0.54 – 4.8 m
18 – 26.5 GHz	1.67 – 1.13 cm	1000	Miteq 2	Octave Horn 1	0.054	35 – 52 cm
26.5 – 40 GHz	1.13 – 0.75 cm	1000	Miteq 3	Octave Horn 2	0.034	21 – 31 cm
40 – 50 GHz	0.75 – 0.60 cm	1000	Miteq 4	Octave Horn 3	0.024	15 – 19 cm
50 - 60 GHz	0.60 – 50 cm	1000	Miteq 4	Octave Horn 3	0.024	19 – 23 cm

*10 kHz – 18 GHz RBW are 6 dB widths whereas 18 – 60 GHz widths are 3 dB widths (taken using Agilent 8565EC analyzer); 3 dB widths are broader than the 6 dB widths of the same numerical value bandwidth by a factor of 1.47.

**Greater of 3λ or $2L^2/\lambda$ where L is the largest antenna dimension [2].

Emission data were recorded for a given antenna for all four thruster operating points before changing the antenna. Below 18 GHz, all four operating points were recorded and the antenna orientation was rotated 90^o to the other polarization before cycling through the four thruster modes again; whereas above 18 GHz, both polarizations were recorded for each thruster operating mode before moving to the next mode.

MIL-STD RE102 (10 kHz – 18 GHz)

Figure 4 display results from the RE102 measurements. These data have not been modified by the anechoic room correction terms shown in Figure 2 which are significant between 20 and 250 MHz. The figure displays the receiver noise (50 ohm load), background, data, and the 461E limit line. The background was taken with all laboratory equipment operating except the thruster. The high background in the 10 – 200 MHz region is due to leakage from the main vacuum tank through the fiberglass tank port into the anechoic room. This background is variable and has been reduced using a carbon fiber mesh over the port. This background does not appreciably contribute to the displayed thruster emission because the ordinate is a logarithmic scale. Observations from these spectra include:

- From 30 MHz to 18 GHz the vertically polarized emission from the thruster is somewhat but not significantly greater than horizontally polarized emission (note results from Figure 2 and both the differences in both the ordinate and abscissa scales when comparing the two polarization data sets);
- emission is notably greater when the thruster is operated at 400 V than when operated at 300 V at all frequencies between10 kHz and 10 GHz;
- emission exceeds the MIL-STD 461E limit line at all frequencies below 300 MHz and between 1 and 4 GHz for both polarizations.

There is a close correlation between the radiated and the anode current oscillations below 10 MHz as discussed below.

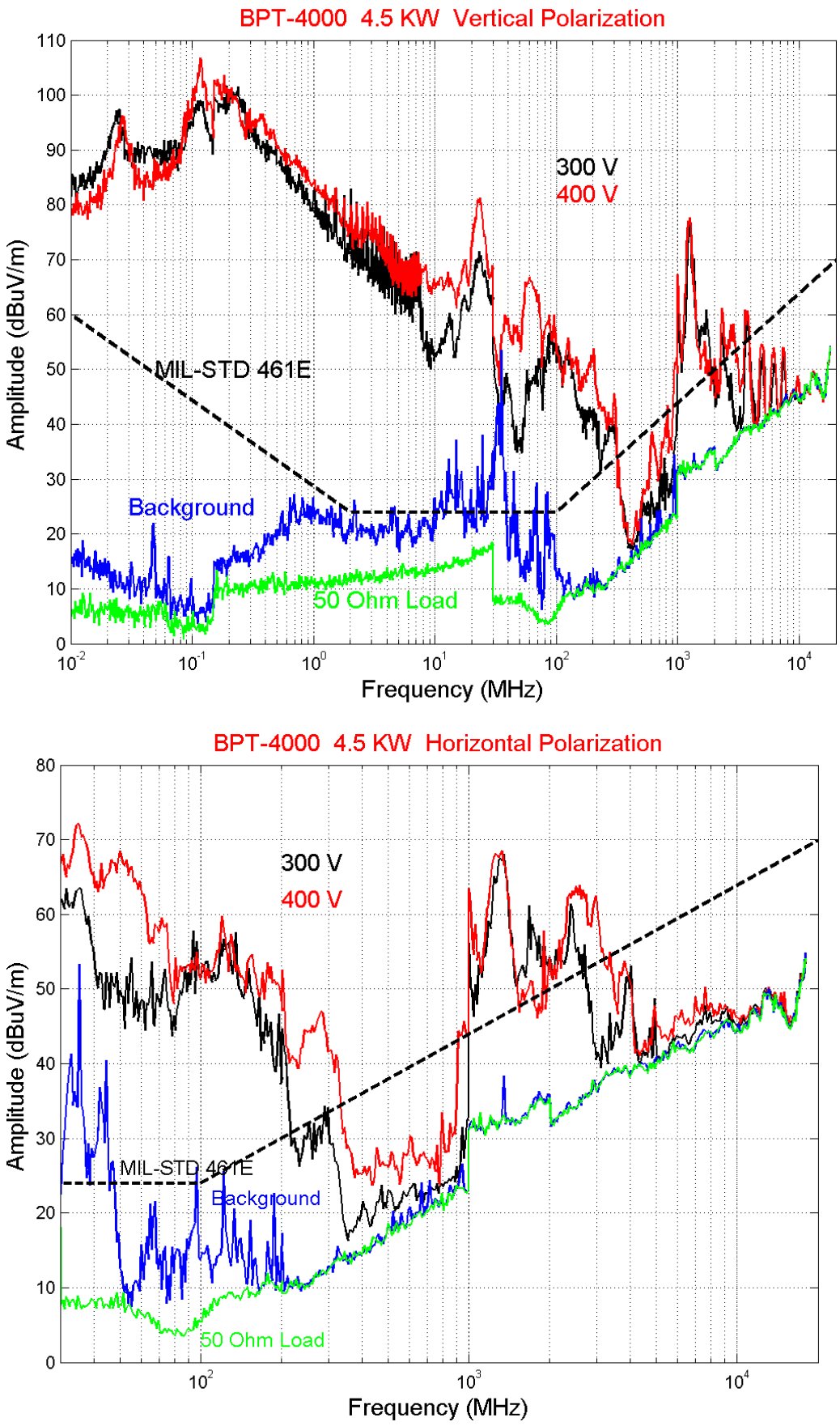

Figure 4. Vertically and horizontally polarized emission spectra from BPT-4000 operating at 4.5 kW.

Electric Field Emission (18 GHz – 60 GHz)

There is increasing interest in satellite communication frequencies above 18 GHz. Accordingly, emission was measured using the four frequency intervals shown in Table 2 employing a newly developed system. The accuracy of this system was measure to be ±1 dB μV/m to a frequency of 40 GHz, the highest frequency for which a calibrated signal generator was available.

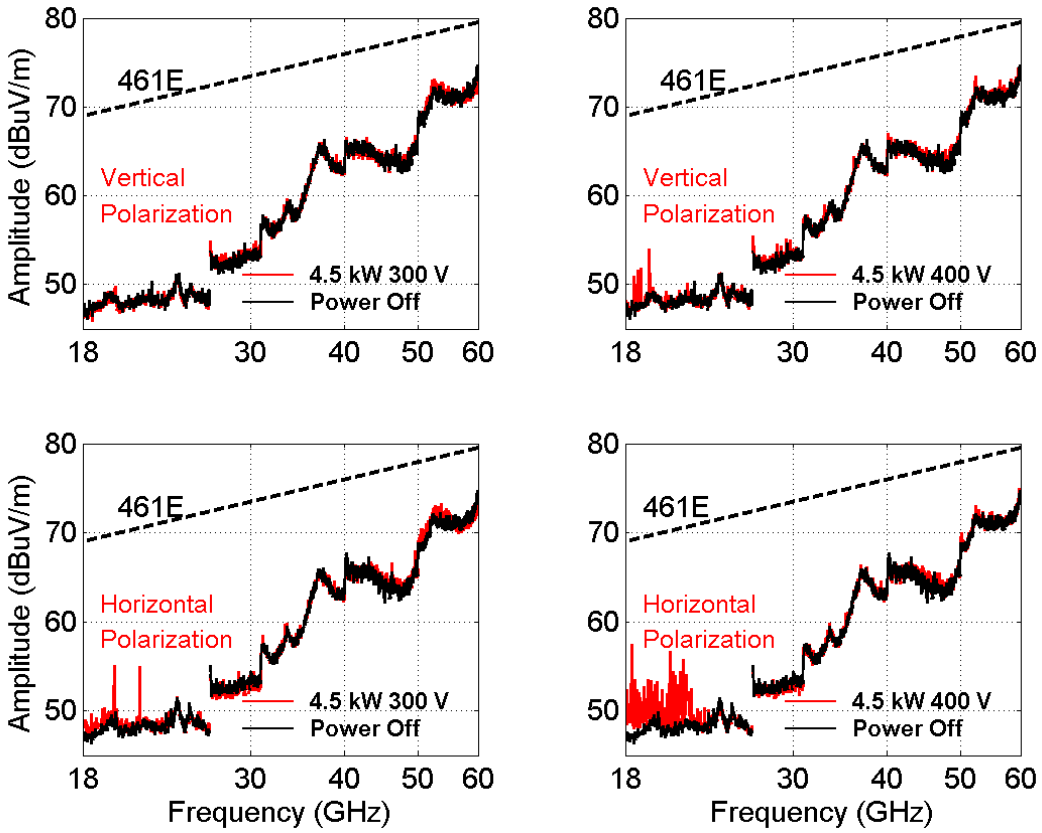

Figure 5. Vertically and horizontally polarized emission from BPT-4000 operating at 4.5 kW between 18 and 60 GHz.

The results of these measurements when the BPT-4000 was operated at 4.5 kW are shown in Figure 5 As expected there is little emission above 18 GHz and no emission above 26 GHz. Between 18 and 26 GHz horizontally polarized emission is greater than vertically polarized emission and emission increases considerably when the discharge potential is increased from 300 to 400 volts. Note that this radiation is at least 10 dB below the projected MIL-STD 461E limit line (slope = 20 dB/decade). Expanded views of this emission are presented in Figure 6.

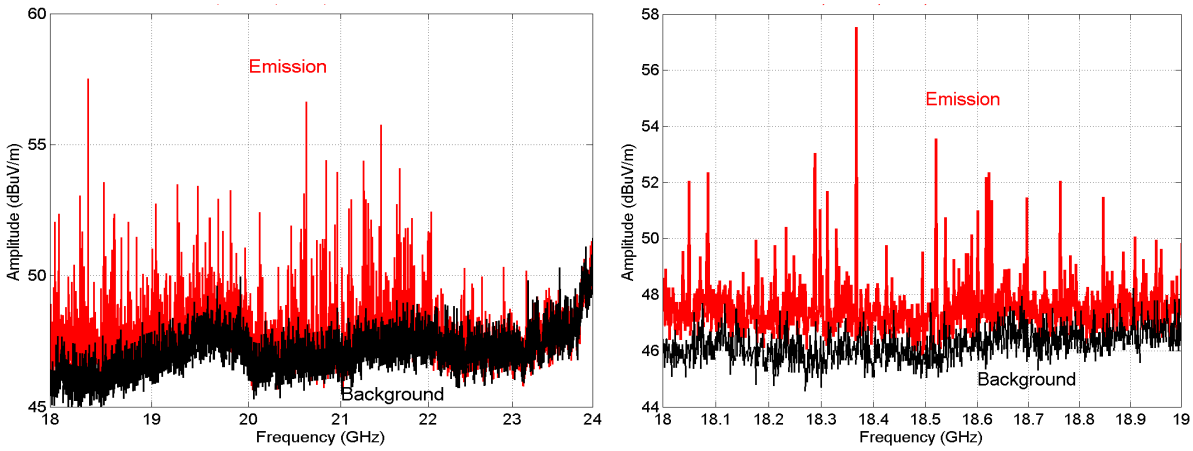

Figure 6. Expanded views of horizontally polarized emission spectra from BPT-4000 operating at 4.5 kW and 400 V.

The radiation above 20 GHz is likely generated when electrons in a plasma are displaced from the uniform background of ions creating a restoring force. This plasma frequency, ν_{pe}, is given by [3]

$$\nu_{pe} = \frac{1}{2\pi}\sqrt{\frac{n_i e^2}{m_e \varepsilon_0}} \cong 9\sqrt{n_i\,(\mathrm{m}^{-3})} \cong 24\ GHz$$

Where the ion density n_i = 7.5 10^{18} m^{-3} for the BPT-4000 operating at 4.5 kW and 400 V, ε_0 = 8.85 x 10^{-12} F/m and e and m_e are the electron charge and mass respectively.

AC Magnetic Field Emission (30 Hz – 300 kHz)

Radiated ac magnetic fields were measured to the side and back of the thruster for three orthogonal transducer orientations (x, y, z) following RE101 of MIL-STD 461D. Only data taken to the side of the thruster is presented here. The distance from the center of the 13.3 cm diameter coil transducer to the center of the thruster was 52.5 cm for the side measurements (the closest accessible position) and 50.0 cm for the rear measurements. MIL-STD 461D allows measurements 7 cm and/or 50 cm from the EUT with limit lines

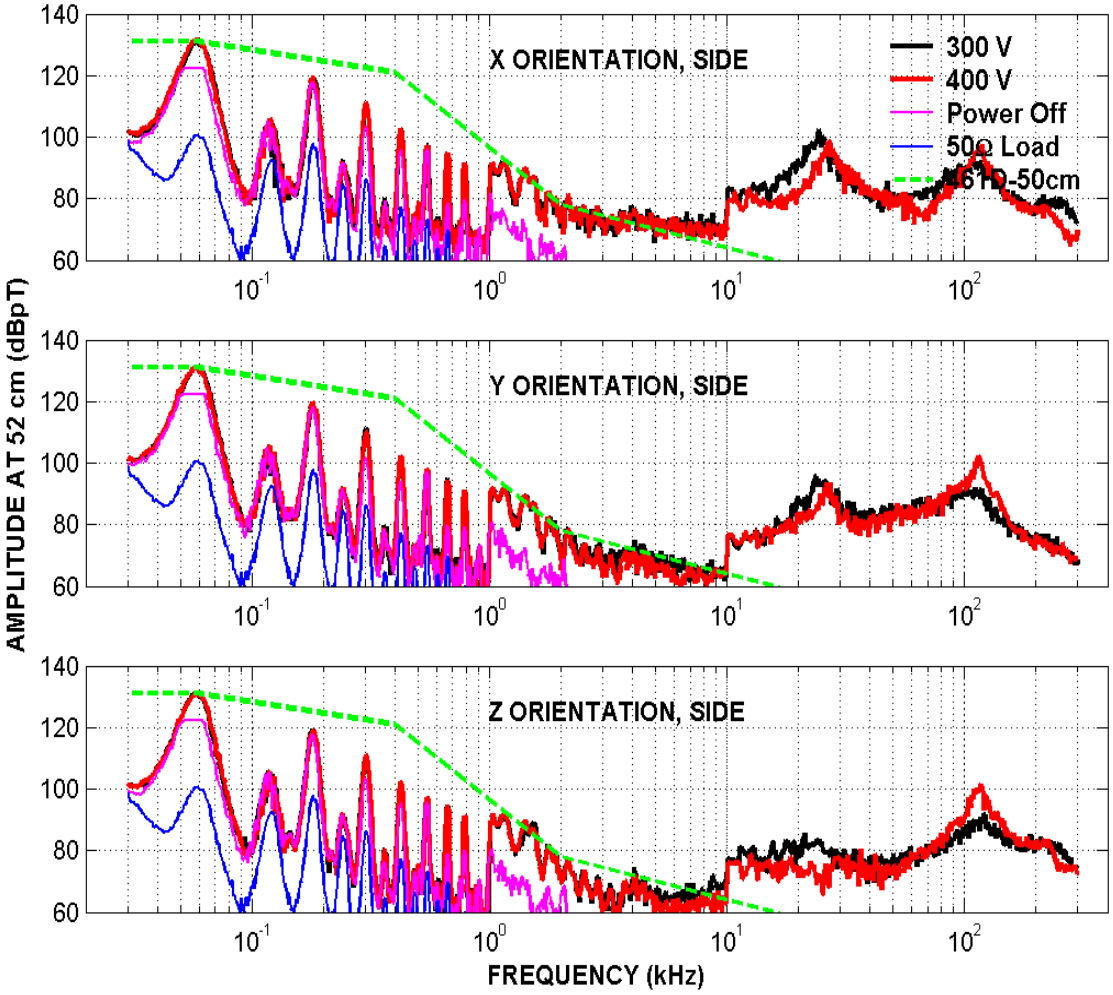

Figure 7. AC magnetic field at 52 cm to the side of the BPT-4000 operating at 4.5 kW. Orientations: X = coil axis horizontal and normal to thruster axis; Y = coil axis horizontal and parallel to thruster axis; Z = coil axis vertical.

for the two separations following an inverse square distance scaling. The frequency measurement was extended to 300 kHz from the MIL-STD limit of 100 kHz. The bandwidths used for these measurements were: 30 Hz - 1000 Hz: 10 Hz; 1 kHz - 10 kHz: 100 Hz; 10 kHz - 300 kHz: 1000 Hz. Magnetic field spectra for the side position and two operating conditions are presented in Figure 7. MIL-STD-461D 50 cm limits are indicated on each plot. Emission exceeds background only above 1 kHz and exceed MIL-STD 461D limits by more than 20 dB above 10 kHz. for all field directions and both discharge potentials. There is little difference in emission for the two discharge potentials at the 4.5 kW power.

Static Magnetic Field Measurements

Static magnetic field measurements were performed using a tri-axial magnetometer (Honeywell HMR2300) mounted outside of the dielectric tank on a rotating arm. The axis of rotation coincided with the thruster exit plane. Angular scans were performed in the thruster mid-plane at three radial distances (66.8, 77.0, 87.2 cm) with four angular positions relative to thruster centerline (45°, 90°, 135°, 180°). At each position the fields at four thruster operating points were measured before proceeding to the next position to allow uniform comparisons. Definitions of the magnetometer axes are shown in Figure 8(a). Note that these axes rotate with the magnetometer and hence are not fixed in the laboratory frame.

Magnetometer data were recorded under conditions that differed in two respects from the other field measurements. First, there was no possibility of keeping the thruster at steady-state temperature given the short burn times needed to cover all positions and operating points. Second, temporary facility restriction made it necessary to operate with five cryopumps rather than seven, so the background pressures were proportionally higher.

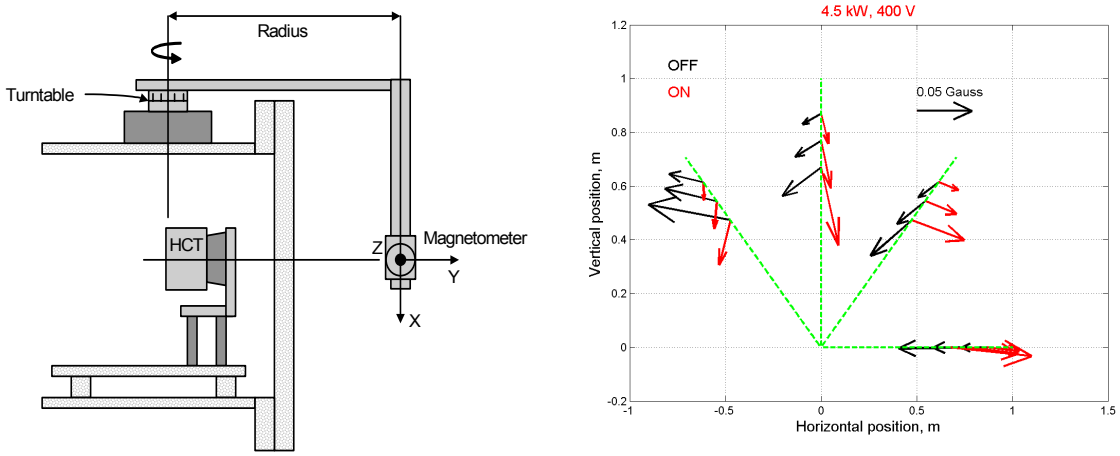

Figure 8. (a) Magnetometer setup shown with probe at 180° from thruster centerline and (b) plot of field for discharge off (magnetic field on) and discharge on.

The nominal calibration factor (15,000 counts per gauss) was confirmed with a laboratory gaussmeter that matched the HMR2300 to within ± 7% under ambient field conditions. Each data file contained a time-resolved record of the tri-axial field at one position and one operating point, including the thruster start transient, steady-state burn, and post-burn operation of the magnet power supply at 7.0 A. This allowed an evaluation of the field with and without the discharge. A data rate of 60 samples per second was used. Field measurements are represented as a vector plot in Figure 8(b) for a 400 V discharge potential. Significant changes in magnitude and direction of the filed (filed reversal exist between the magnet on/discharge current off and magnet on/discharge current off conditions. For a given power, there is no significant change in the field with a change in the discharge voltage.

Conducted Emissions

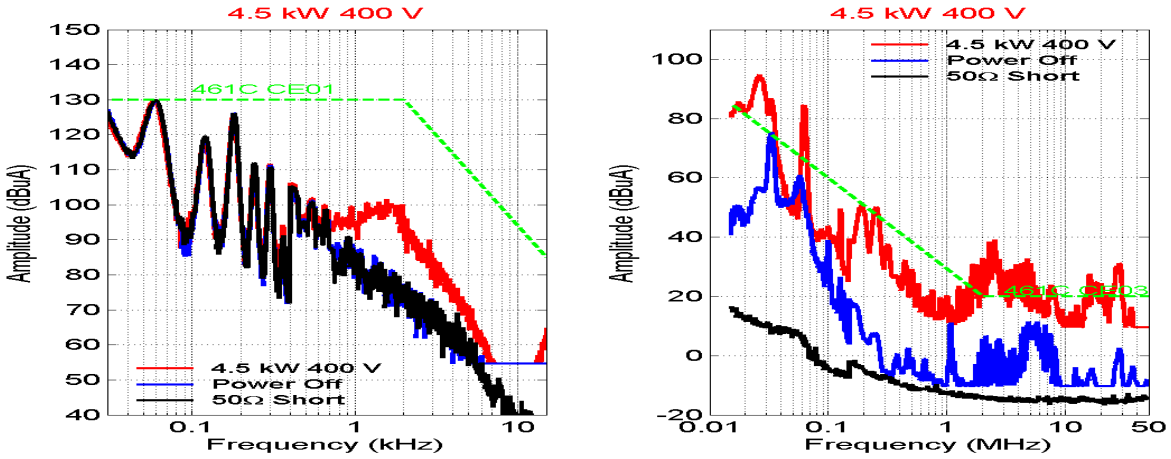

Figure 9. CE01 and CE03 conducted emissions for 4.5 kW and 400 V.

Conducted emissions were recorded using MIL-STD 461C CE01 and CE03 specifications except that the CE03 upper frequency limit was extended to 50 MHz. The measurements were taken using an ETS Model 91550-1L Current Probe (20Hz – 100 MHz). Three 10 µF shunting capacitors were used to reduce high frequency current from the bus simulator and the PPU. The current probe encircled these three lines near the PPU. Figure 9 displays the CE01 and CE03 data for the BPT-400 operating at 4.5 kW and 400 volts. There was no significant difference between the 300 and 400 volt data at 4.5 kW. Below 10 kHz there is little conducted emission but 1 MHz there are amplitudes as much as 20 dB above MIL-STD 461C limits.

Discharge Current Oscillations

Discharge current oscillations are believed to be closely linked to the pattern of radiated emissions. A series of tests was performed to explore the spectra of these oscillations as a function of thruster operating conditions. The objective of these tests was to determine the sensitivities of the measured spectra to discharge voltage and power, power source (laboratory supply or PPU), and cabling in order to identify those operating conditions which minimize these oscillations.

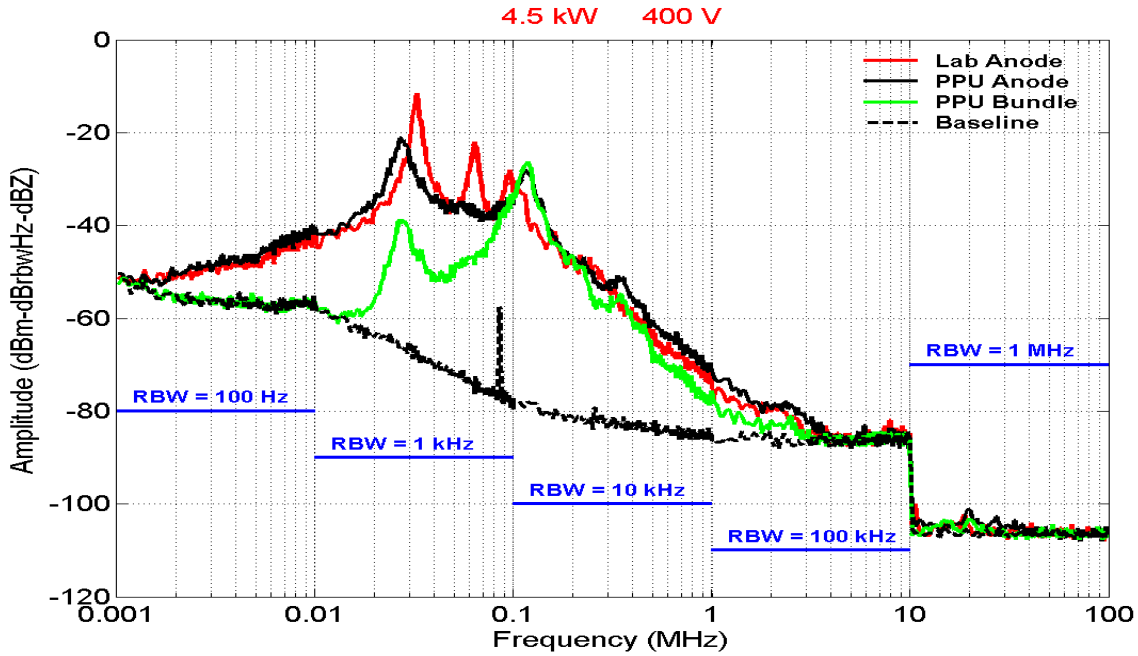

Figure 10. Spectra of current oscillations (4.5 kW, 400 V). The resolution bandwidths (RBW) are indicated.

A clip-on Prodyn Technologies I-125-4A current probe was attached to an exposed section of the cable between the PPU output and the vacuum feedthrough. The signal from the current probe was fed as an input to a Tektronix 2755AP spectrum analyzer. At each of the thruster operating conditions the signal was sampled in one-decade frequency increments. The data were post-processed by normalizing the measured signal by the corresponding resolution bandwidth and then correcting for the probe impedance. The representative results shown in Figure 10 represent dBm (50 ohm) per unit resolution bandwidth normalized to a probe impedance of 1 ohm.

Three test configurations were studied: 1) the anode cable through the transducer with the thruster powered with the laboratory power supplies; and 2) the anode cable through the transducer with the thruster powered by the PPU; 3) the entire cabling bundle through the transducer with thruster powered by the PPU. The current oscillation spectra for these configurations with the thruster operating a 4.5 kW and 400 V is presented in Figure 10. The main features in these spectra include a primary peak in the vicinity of 30 kHz with harmonics at 60 and 90 kHz overlying an incoherent background extending from 1kHz to 1MHz. Much weaker features are observed near 2 and 20 MHz. In general, the signal from the bundle is weaker than that from the anode alone at the lower frequencies. This is presumably because the bundle has currents flowing in both directions, canceling some of the field from the anode current. Compared with current from thruster when operated by laboratory power supplies, the currents from the thruster powered by the PPU are somewhat reduced and broadened, the peak near 60 kHz is eliminated.

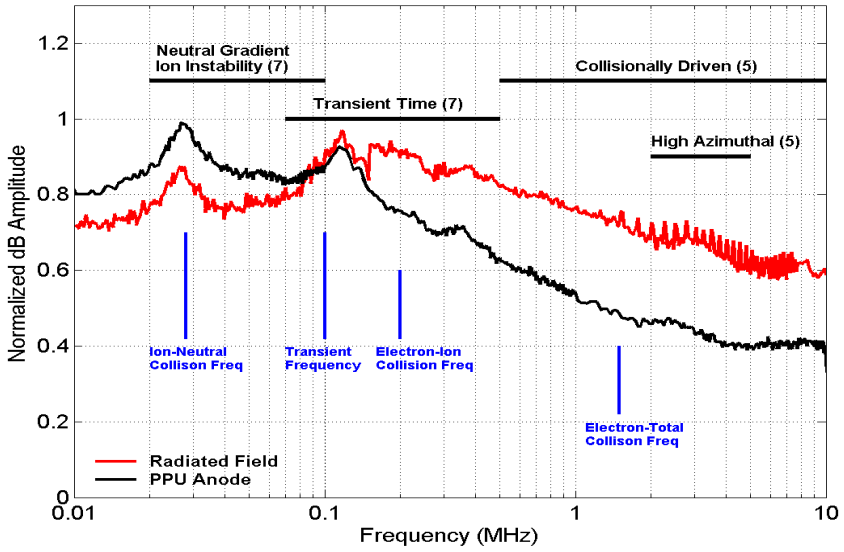

Figure 11. Spectra of current oscillations at 4.5 kW and 400 V.

Figure 11 displays a comparison of the anode oscillations and radiated electric field when the BPT-4000 is operated by the PPU. The two spectra show similar peaks near 28 and 120 kHz and have approximately the same slope at higher frequencies (oscillations are apparent in the radiated field and not in the current above 1 MHz likely because the resolution bandwidth was 10 times greater for the current measurements). During the 1970s, several studies of low frequency oscillations (< 400 MHz) were made in Russia identifying six regions of Hall thruster operation classified by magnetic field strength. These operating regions had different spectral profiles that were divided into seven frequency zones, each zone with a strength marked on a 0 –10 scale. [4] These oscillations were analyzed by Choueiri [5] who associated physical processes with each frequency zone. These zones, strengths, and processes are identified on Figure 11 for a thruster operating at optimal magnetic field strength. Characteristic frequencies of the plasma are also marked. The understanding of these current oscillations that give rise to the radiated fields in this frequency region is good but not complete.

DISCUSSION

Hall thrusters generate significant radiation from frequencies of tens of Hz to tens of GHz. This radiation must be quantitatively characterized for all expected operating modes of the thruster before it can be integrated to a satellite bus. Although radiation from the BPT-4000 Hall thruster is characteristic of that seen from other Hall thrusters, each thruster has its own emission spectrum and this spectrum changes with operating mode. For the operating modes of the BPT-4000 EDM studied here, the highest intensity is seen at frequencies below 1 MHz where the radiated electric field correlates well with anode current oscillations. Electric field radiation decreases quasi -monotonically between 200 kHz and 400 MHz with relative peaks near 20 and 60 MHz. Radiation sharply increases near 1 GHz with measurable emission to near 25 GHz for some operating conditions. AC magnetic field radiation is significant above a few kHz to 300 kHz, the highest frequency measured here. Conduced emissions were not significant below 10 kHz, but could be important above this frequency. Aside from their importance for integration issues, measurements such as these may prove to be important to assess the on-board health of a thruster. This may be especially true at frequencies above 1GHz where this identification has already been made. [6] For diagnostic applications, measurements for expected as well and unexpected operating conditions could prove to be valuable.

ACKNOWLEDGEMENT

Steve Meyer, Chris Rayburn, Lee Silberkleits, Kristi DeGrys and Jack Fisher of Aerojet made significant contributions to this project.

REFERENCES

1. E. J. Beiting, "Design and Performance of a Facility to Measure Electromagnetic Emissions from Electric Satellite Thrusters," AIAA-2001-3344, 37th AIAA/ASME/SAE/ASEE Joint Propulsion Conference & Exhibit, 8-11 July 2001,Salt Lake City, Utah.
2. C. R. Paul, *Introduction to Electromagnetic Compatibility*, John Wiley & Sons, New York, 1992.
3. R. N. Franklin, *Plasma Phenomena in Gas Discharges*, Clarendon Press, Oxford, 1976, p15.
4. G. N. Tilinin, "High-frequency plasma waves in a Hall accelerator with an extended acceleration zone," *Soviet Physics, Technical Physics* **22**(8), 974-978, 1977.
5. E. Y. Choueiri, "Plasma Oscillations in Hall Thrusters," *Phys. Plasmas*, **8**(4), 1411-1426 (2001).
6. V. I. Brukhty and K. O. Kirdyashev, "Microwave Oscillations as an Indicator of Anomalous Wall Erosion in SPT Accelerating Chamber," 26 International Electric Propulsion Conference, 17-21 October 1999, Kitakyushu, Japan.